Journal of
Materials Chemistry

Cite this: *J. Mater. Chem.*, 2012, **22**, 16269

www.rsc.org/materials

PAPER

Tracking of high-temperature thermal expansion and transport properties *vs.* oxidation state of cobalt between +2 and +3 in the $La_2Co_{1+z}(Ti_{1-x}Mg_x)_{1-z}O_6$-system

S. Shafeie,*[a] J. Grins,[a] S. Ya. Istomin,[b] A. A. Gippius,[b] L. Karvonen,[c] S. Populoh,[c] A. Weidenkaff,[c] J. Köhler[d] and G. Svensson[a]

Received 23rd April 2012, Accepted 24th June 2012
DOI: 10.1039/c2jm32550k

The high-temperature thermal expansion and electronic transport properties of the B-site substituted $LaCoO_3$ with both variable oxidation state of cobalt between +2 and +3 ($La_2Co(Ti_{1-x}Mg_x)O_6$, $0 \le x \le 0.5$) and variable Co^{3+}-content relative to the other B-cations ($La_2Co_{1+z}(Ti_{0.5}Mg_{0.5})_{1-z}O_6$, $0.2 \le z \le 0.6$) have been investigated. Based on the temperature dependence of the thermal expansion, electronic transport properties and Seebeck coefficient, three different groups of compositions according to their symmetries can be allocated. It was found that the thermal expansion coefficients (TECs) of the studied compounds are mainly dependent on the proportion of Co^{2+}/Co^{3+}. For $La_2Co(Ti_{1-x}Mg_x)O_6$, the TEC increases from ~9 ($x = 0$) to ~19 ppm K^{-1} ($x = 0.5$) with an increase of the oxidation state of cobalt from +2 to +3, respectively. The TECs of $La_2Co_{1+z}(Ti_{0.5}Mg_{0.5})_{1-z}O_6$, $z = 0.2$–0.6 with Co^{3+}-only, remain constant at ~21 ppm K^{-1} independent of the cobalt content. Thermoelectric measurements of the system indicate that all samples in the system, except $La_2Co_{1.6}(Ti_{0.5}Mg_{0.5})_{0.4}O_6$, are p-type conductors over the whole temperature range, $300 < T < 1175$ K. The conductivities were found to increase with an increase of both Co^{3+} and total cobalt content and are described with a small polaron hopping model. Due to an insignificant number of oxygen vacancies of $La_2Co_{1+z}(Ti_{1-x}Mg_x)_{1-z}O_6$ samples prepared in air at elevated temperatures, the investigated system is proposed as an excellent model system for the investigation of the influence of the Co oxidation state and stoichiometry on different properties in perovskite cobalt oxides.

1. Introduction

The perovskite type cobaltate $LaCoO_3$ (LCO) has been the object of many studies[1–6] due to its complex magnetic and electronic transport properties caused by transitions between different spin states of Co^{3+}. For example, $LaCoO_3$ undergoes a spin-state transition from low spin (LS, $t_{2g}{}^6e_g{}^0$) to high spin (HS, $t_{2g}{}^4e_g{}^2$) at about 100 K leading to a change from a diamagnetic to a paramagnetic behaviour. Above 500 K its conductivity transcends from a semiconducting to a metallic conductivity. Starting from the theoretical work of Korotin *et al.*[7] in which a stabilization of an excited intermediate spin state (IS, $t_{2g}{}^5e_g{}^1$) was proposed, a number of studies claiming the presence of IS Co^{3+} in $LaCoO_3$ are found in the literature.[8–10] However, the existence of IS Co^{3+} in perovskite-related cobaltates is now widely accepted although some studies support the LS/HS state scenario, *e.g.* X-ray absorption spectroscopy shows only LS and HS Co^{3+} in $LaCoO_3$ up to 650 K.[11] Temperature-induced spin state transitions of Co^{3+} resulted in high thermal expansion coefficients (TECs) of cobaltites (*e.g.* $TEC_{LaCoO_3} \approx 21$ ppm K^{-1} (ref. 12 and 13)) and significantly hamper their use in solid oxide fuel cells (SOFCs) and gas separation membranes.[13,14] Therefore, it is of great interest to study the influence of the oxidation state of cobalt on high-temperature thermal expansion and electronic conductivity properties of Co-containing perovskites.

Recently, we have reported on the phase formation and structural characterization of perovskite phases in the system $La_2Co_{1+z}(Ti_{1-x}Mg_x)_{1-z}O_6$ ($0 \le x \le 1$, $0 \le z \le 1$).[15] For $La_2Co(Ti_{1-x}Mg_x)O_6$ ($0 \le x \le 0.6$) being compounds with fixed cobalt content, the formal Co oxidation state is changed from +2 to +3.2 with a substitution of Ti^{4+} by Mg^{2+}. The symmetry of the perovskite phase in the system changes from monoclinic ($P2_1/n$) for $0 \le x \le 0.2$ *via* orthorhombic ($Pnma$) ($0.3 \le x \le 0.4$) to rhombohedral ($R3c$) ($0.5 \le x \le 0.6$). Rhombohedral perovskites $La_2Co_{1+z}(Ti_{0.5}Mg_{0.5})_{1-z}O_6$ ($0 \le z \le 0.6$) with a fixed formal oxidation state of +3 for Co and the Co concentration at the B site between 50 and 80% were also synthesised. In this study, we present

---

[a] *Department of Materials and Environmental Chemistry, Stockholm University, SE-106 91 Stockholm, Sweden. E-mail: ssafe@mmk.su.se*
[b] *M. V. Lomonosov Moscow State University, 119991 Moscow, Russia*
[c] *Laboratory for Solid State Chemistry and Catalysis, EMPA – Swiss Federal Laboratories for Materials Science and Technology, CH-8600 Dübendorf, Switzerland*
[d] *Max Planck Institute for Solid State Research, Heisenbergstraße 1, 70569 Stuttgart, Germany*

high temperature properties of these compounds, *i.e.* thermal expansion, electronic conductivity, Seebeck coefficient and magnetic susceptibility. We discuss how these properties correlate with the structure, oxidation state and absolute amount of cobalt.

2. Experimental

2.1. Synthesis

Samples in the $La_2Co_{1+z}(Ti_{1-x}Mg_x)_{1-z}O_6$ ($z = 0$ and $0 \le x \le 0.5$, step $= 0.1$; $x = 0.5$ and $0 \le z \le 0.6$, step $= 0.2$) system were synthesized by the citric acid route. The starting materials, *i.e.*, La_2O_3 (Aldrich, 99.99%), MgO (Merck, analytical grade) (both powders were pre-dried at 1223 K for 24 h), cobalt(II)acetate tetra hydrate (Sigma-Aldrich, reagent grade) and titanium(IV) butoxide (Sigma-Aldrich, 97.0 wt%) were dissolved in stoichiometric amounts in concentrated nitric acid with anhydrous citric acid (Merck, 99%) as a complex binder to get a well dispersed mixture of the elements in the precursor gel. More details about the synthesis are described in ref. 15. The gels were calcinated at 1173 K in air for 2 h. The samples were annealed in air at a final temperature of 1623 K for 24 h with intermediate grindings.

2.2. Characterization

2.2.1. Thermal expansion. Linear thermal expansion measurements were made on a Netzsch DIL 402C dilatometer calibrated with a sapphire sample as a standard. Oxide powders were pressed into pellets of 8 mm diameter and 5–5.5 mm height and sintered at 1623 K for 24 h in air and polished to approximately the same size as the sapphire standard. Measurements were performed in air from room temperature (RT) up to 1273 K, at a heating rate of 5 K min^{-1}.

2.2.2. High-temperature determination of the Seebeck coefficient and electronic conductivity measurements. The high-temperature Seebeck coefficient and electronic conductivity were measured in synthetic air atmosphere from RT up to 1173 K with an Ozawa Science RZ2001i measurement system. The presented measurements were restricted to the reliable measurement range of electrical resistivities between 10^{-7} and 10^4 Ω m. The electronic conductivity was measured using the four-point probe method, while the Seebeck coefficient was measured in steady-state mode. Samples were prepared in the form of rectangular bars with dimensions 2 mm × 2 mm × 13 mm and sintered again using the same program as with the initial synthesis.

2.2.3. High temperature magnetic properties. Temperature dependence measurements of the magnetic moment in the temperature range from RT to 800 K at an applied magnetic field of 1 T of the pressed powder samples of $La_2Co_{1+z}(Ti_{1-x}Mg_x)_{1-z}O_6$ were performed using a MPMS SQUID magnetometer (Quantum Design).

3. Results

3.1. Thermal expansion

Thermal expansion curves, from RT up to 1273 K, for $La_2Co(Ti_{1-x}Mg_x)O_6$ ($0 \le x \le 0.5$) and $La_2Co_{1+z}(Ti_{0.5}Mg_{0.5})_{1-z}O_6$ ($0 \le z \le 0.6$) are shown in Fig. 1a and b, respectively. Only the La_2CoTiO_6 ($x = 0$) sample, nominally containing only Co^{2+}, expands linearly with temperature. For all other samples, the curves are sigmoidal with an increase of TEC with temperature. For $La_2Co_{1+z}(Ti_{0.5}Mg_{0.5})_{1-z}O_6$ ($0 \le z \le 0.6$) samples (see Fig. 1b) the curves have similar shapes and are practically identical for $z = 0.2$, 0.4 and 0.6. The average TEC calculated between $T = 298$ and 1173 K is given in Fig. 2.

3.2. High temperature electronic conductivity

The temperature dependence of the d.c. electronic conductivity between RT and 1173 K was measured in synthetic air, both for $La_2Co(Ti_{1-x}Mg_x)O_6$ ($0 \le x \le 0.5$) and $La_2Co_{1+z}(Ti_{0.5}Mg_{0.5})_{1-z}O_6$ ($0 \le z \le 0.6$). All the samples showed an increase in conductivity (σ) with increasing temperature. The semiconductor-like behaviour of these samples and the results from XANES measurements[15] indicate that the cobalt ions exist in two discrete oxidation states, *i.e.* +2 and +3, and suggest that the electronic conduction in these samples can be described in terms of a small polaron hopping model. The conductivity increases with the increase of the Co^{3+} content for $La_2Co(Ti_{1-x}Mg_x)O_6$ ($0 \le x \le 0.5$) and with the increase of the total

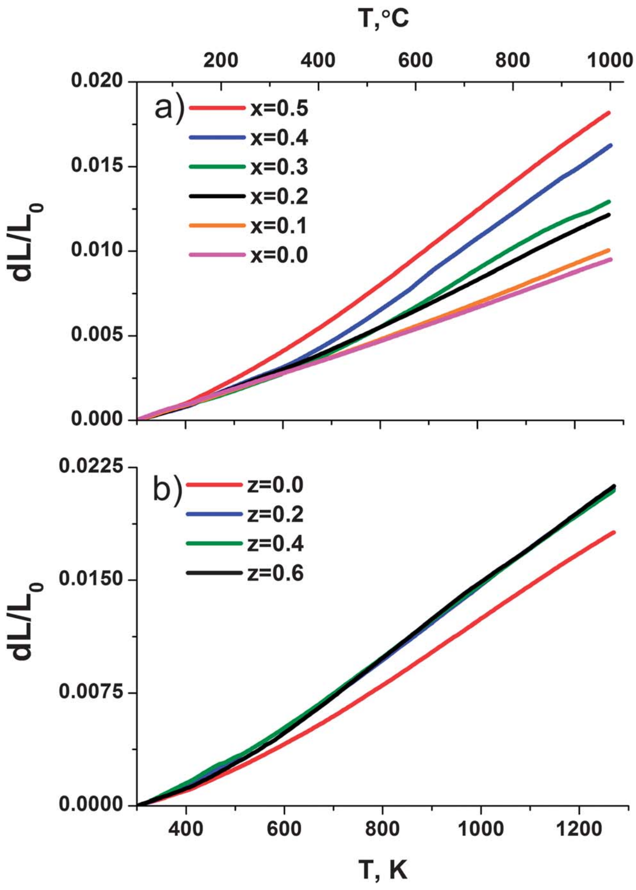

Fig. 1 Linear thermal expansion for (a) $La_2Co(Ti_{1-x}Mg_x)O_6$ ($0 \le x \le 0.5$) and (b) $La_2Co_{1+z}(Ti_{0.5}Mg_{0.5})_{1-z}O_6$ ($0 \le z \le 0.6$). The bottom curve corresponds to $x = 0$ and $z = 0$ in (a) and (b), respectively, thereafter they follow with increasing values to the uppermost curve with the x and z values.

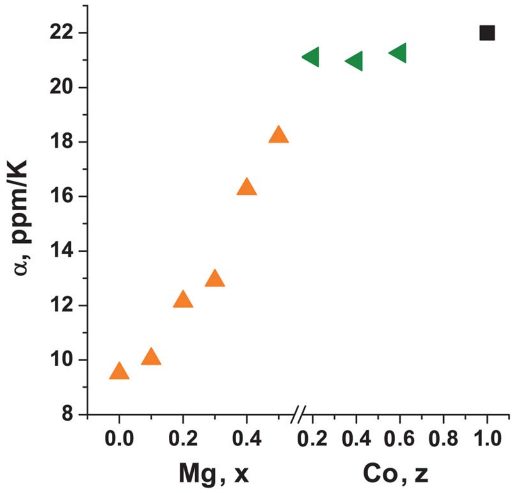

Fig. 2 Average linear thermal expansion coefficient (TEC) at temperatures 298–1273 K (left) for $La_2Co(Ti_{1-x}Mg_x)O_6$ as a function of x and (right) for $La_2Co_{1+z}(Ti_{0.5}Mg_{0.5})_{1-z}O_6$ as a function of z. The value for $LaCoO_3$ has been inserted as a reference (black square).[16]

amount of Co^{3+} for $La_2Co_{1+z}(Ti_{0.5}Mg_{0.5})_{1-z}O_6$ ($0 \leq z \leq 0.6$). The graphs of $\log(\sigma T)$ *vs.* $1/T$ for the studied samples are shown in Fig. 3. For $x = 0.0$ and 0.1, a smooth, nearly linear Arrhenius-type behaviour is observed. For $La_2Co(Ti_{1-x}Mg_x)O_6$ with an increase of the Co^{3+} content (x), the slope of the curves starts to decrease at higher temperatures, $T > 673$ K, indicating a decrease in the activation energy. This behaviour becomes even more pronounced and shifted towards lower temperatures for $La_2Co_{1+z}(Ti_{0.5}Mg_{0.5})_{1-z}O_6$ ($0 \leq z \leq 0.6$) containing only Co^{3+}.

The activation energies for the conduction have been derived from the nearly linear regions between 473 and 873 K using the Arrhenius like equation modified for small polarons:

$$\sigma = \frac{\sigma_0}{T} e^{-E_\sigma / k_B T} \qquad (1)$$

where σ is the electronic conductivity, T the absolute temperature, k_B Boltzmann's constant, σ_0 a pre-exponential factor containing information about the charge carrier concentration and their mobility and E_σ the activation energy. Calculated values of E_σ and conductivity σ of the samples at $T = 1173$ K for $La_2Co(Ti_{1-x}Mg_x)O_6$ and $La_2Co_{1+z}(Ti_{0.5}Mg_{0.5})_{1-z}O_6$ are shown in Fig. 4. The activation energies for the electronic conductivity lie around 0.5 eV for Co^{2+}-rich compositions ($x = 0.0$ and 0.1), while a significant higher value ~0.65 eV is observed for $x = 0.2$, whereafter it decreases to ~0.45 eV for $x = 0.5$. The increase of the total amount of Co^{3+} at the B-site along the z-line decreases the activation energy towards $E_\sigma \approx 0.25$ eV as reported for $LaCoO_3$ between 373 and 1273 K (ref. 17).

3.3. Seebeck coefficient measurements

The Seebeck coefficients, S ($\mu V\ K^{-1}$), were measured between RT and 1173 K in synthetic air for the samples $La_2Co(Ti_{1-x}Mg_x)O_6$ ($0 \leq x \leq 0.5$) and $La_2Co_{1+z}(Ti_{0.5}Mg_{0.5})_{1-z}O_6$ ($0 \leq z \leq 0.6$) as shown in Fig. 5. The Seebeck coefficients for all the $La_2Co(Ti_{1-x}Mg_x)O_6$ samples with a variable nominal oxidation state of cobalt are positive with $S > 100\ \mu V\ K^{-1}$ at all the temperatures measured, which is typical for a small polaron conductor.[18] The positive sign indicates that holes are the major charge carriers. For all the studied compositions the temperature dependence of the Seebeck coefficient stabilises or even converges to an approximately constant value at higher temperatures. Such a phenomenon is common in systems where a charge disproportionation takes place, *i.e.* $2Co^{3+} \rightarrow Co^{2+} + Co^{4+}$.[17] Selecting a conduction model assuming small polarons as charge carriers can be supported by quantifying the heat of charge carrier jump $H_\pm$ (unit in eV)[19] for the different compositions, which can be calculated from $H_\pm = E_\sigma - E_S$. The energy of polaron ionization E_S is calculated from the Seebeck coefficient according to the formula:[20]

$$S = \pm \frac{k_B}{e}\left(\frac{E_S}{k_B T} + B\right) \qquad (2)$$

where E_S is the energy of polaron ionization, e the charge of the electron and B an entropy term for the charge transfer (where E_σ is the activation energy from the electronic conductivity measurements discussed above). $H_\pm \neq 0$ is an indication of

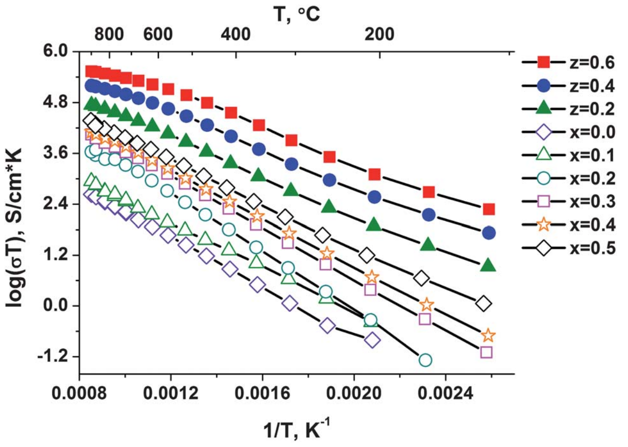

Fig. 3 Arrhenius plot of the high temperature electronic conductivity data $\log(\sigma T)$ *vs.* $1/T$ of $La_2Co(Ti_{1-x}Mg_x)O_6$ ($0 \leq x \leq 0.5$) and $La_2Co_{1+z}(Ti_{0.5}Mg_{0.5})_{1-z}O_6$ ($0 \leq z \leq 0.6$).

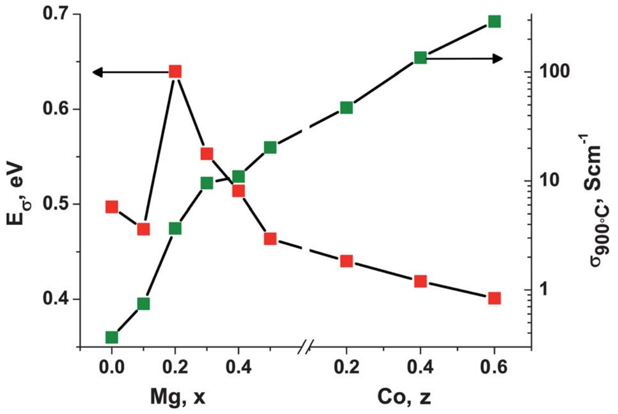

Fig. 4 The variation of the electronic conductivity at $T = 1173$ K (green symbols) and the corresponding activation energies (red symbols) for the compositions $La_2Co(Ti_{1-x}Mg_x)O_6$ ($0 \leq x \leq 0.5$) and $La_2Co_{1+z}(Ti_{0.5}Mg_{0.5})_{1-z}O_6$ ($0 \leq z \leq 0.6$).

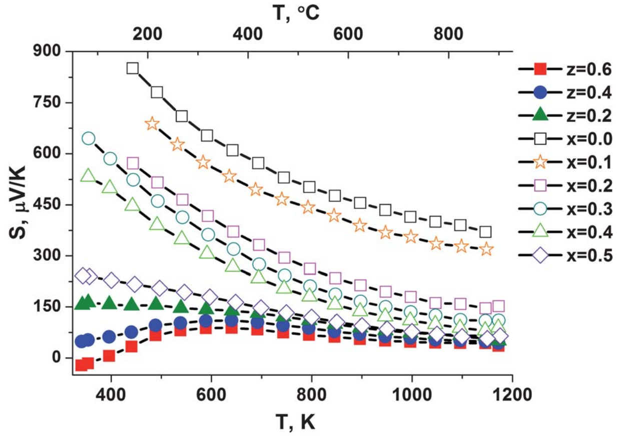

Fig. 5 Seebeck coefficients *vs.* T, measured from RT to 1173 K in air, of $La_2Co(Ti_{1-x}Mg_x)O_6$ ($0 \le x \le 0.5$) and $La_2Co_{1+z}(Ti_{0.5}Mg_{0.5})_{1-z}O_6$ ($0 \le z \le 0.6$).

thermally activated charge transfer of "jumping" localized electrons/holes, *i.e.* small-radius polarons, while for $H_\pm \approx 0$ the charge transfer is more metallic; *i.e.* by large-radius polarons, with zero/very low activation energy.[19] The Seebeck coefficients *vs.* $1/T$ are shown in Fig. 6. The values for E_S are calculated using the linear part in the temperature range $623 \le T \le 1143$ K in Fig. 6 as shown in Fig. 7. The heat of charge transfer jump calculated as $H_\pm = E_\sigma - E_S$ is presented in Fig. 8. The observed values are up to a magnitude larger than that reported for $LaCoO_3$, ~0.07 to 0.085 eV,[19] thus in agreement with a small polaron model.

3.4. High temperature magnetic properties

The high temperature magnetic susceptibilities were measured in air between 300 and 800 K for the $La_2Co(Ti_{1-x}Mg_x)O_6$, $x = 0.0$, 0.2, 0.5 samples in order to follow the changes in the magnetic moment (μ_{eff}) for Co in the nominal oxidation states +2, +2.4 and +3, as shown in Fig. 9 and 10. The $x = 0.0$ and 0.2 samples exhibit a Curie–Weiss law behaviour over the whole measured temperature range while the $x = 0.5$ sample does not. The calculated magnetic moments from the Curie–Weiss law for $x = 0.0$ and $x = 0.2$ are 4.02 and 3.96 B.M., respectively. The value for the $x = 0.0$ sample is close to the expected magnetic moments for Co^{2+} (HS) (3.87 B.M.). A lower value obtained for the $x = 0.2$ sample indicates that some of the Co^{3+} cations are in the LS state. Taking into account the spin-only values for Co^{2+} (HS) and Co^{3+} (HS) and (LS) one can estimate that <84% of Co^{3+} are in the HS state. The calculated μ_{eff} for $x = 0.5$ increases with temperature from ~2.0 B.M. at 300 K to *ca.* 2.8 B.M. at 800 K indicating an increase of the amount HS Co^{3+} at the expense of LS Co^{3+}. It should be noted that the μ_{eff} value at 800 K corresponds to <57% while the μ_{eff} value at 300 K corresponds to <40% HS Co^{3+}.

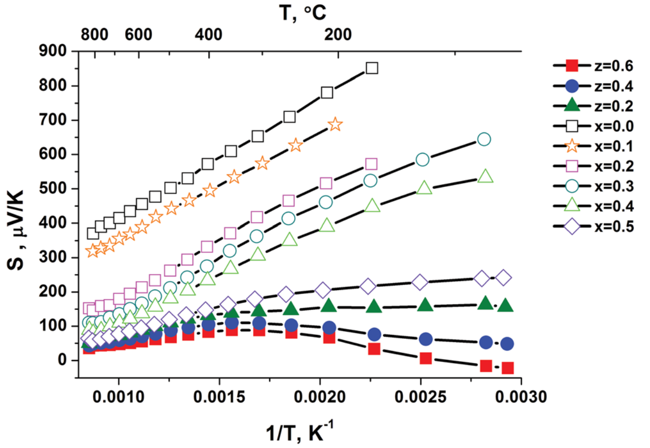

Fig. 6 Seebeck coefficients *vs.* $1/T$, measured from RT to 1173 K in air, of $La_2Co(Ti_{1-x}Mg_x)O_6$ ($0 \le x \le 0.5$) and $La_2Co_{1+z}(Ti_{0.5}Mg_{0.5})_{1-z}O_6$ ($0 \le z \le 0.6$). A linear Arrhenius behaviour is observed in the temperature range ~643 to 1143 K.

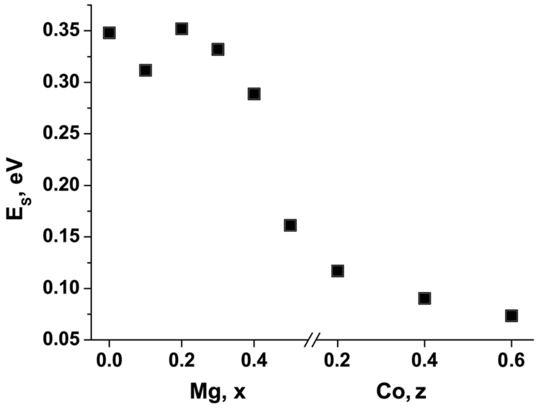

Fig. 7 Corresponding values for the energy of polaron ionization (E_S) calculated from the Seebeck coefficients *vs.* $1/T$ in the linear temperature range ~643 to 1143 K for $La_2Co(Ti_{1-x}Mg_x)O_6$ ($0 \le x \le 0.5$) and $La_2Co_{1+z}(Ti_{0.5}Mg_{0.5})_{1-z}O_6$ ($0 \le z \le 0.6$).

4. Discussion

The number of studies on the correlations between cobalt oxidation state and various high-temperature properties of cobalt-based perovskites is quite limited, probably due to difficulties in controlling the compositions. For example, A-site substituted (A = alkaline-earth cation) $LaCoO_3$ is not suitable

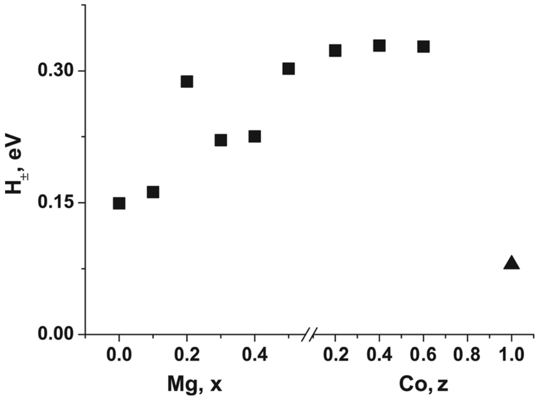

Fig. 8 Compositional variation of the heat of charge carrier jump, $H_\pm$ (eV). The value for $LaCoO_3$ has been inserted as a reference (black triangle).[19]

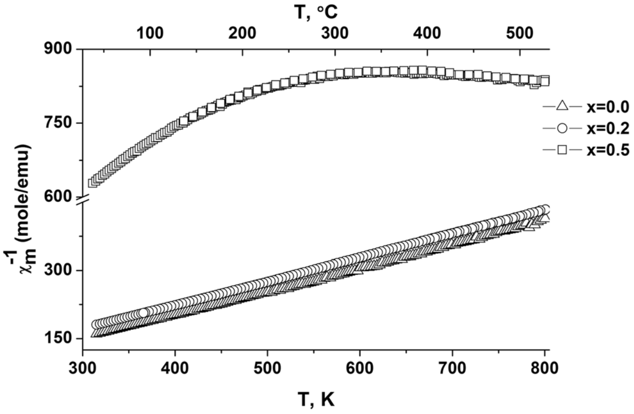

Fig. 9 Temperature dependence of inverse magnetic susceptibilities (χ^{-1}) for $La_2Co(Ti_{1-x}Mg_x)O_6$, $x = 0.0$, 0.2 and 0.5 samples.

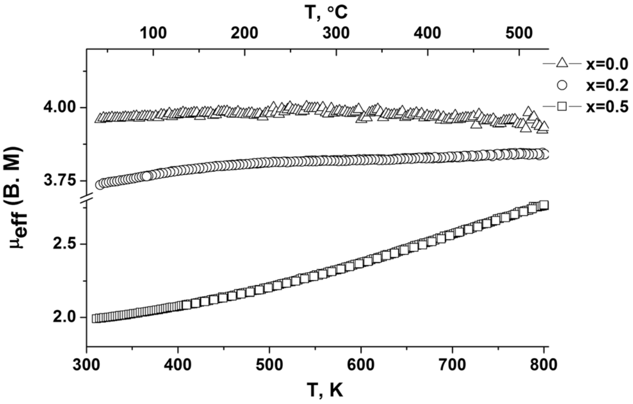

Fig. 10 Temperature dependence of the calculated magnetic moments (μ_{eff}) for $La_2Co(Ti_{1-x}Mg_x)O_6$, $x = 0.0$, 0.2 and 0.5 samples.

for such studies since the oxygen content of the perovskites $La_{1-x}A_xCoO_{3-y}$ changes with both composition (x) and temperature.[13,21] B-site substituted $LaCoO_3$ compounds are better suited, but only when the B cation is in a stable oxidation state *e.g.* Mg^{2+}, Sc^{3+}, Ti^{4+}, since it otherwise can result in an uncertainty in the oxidation state of the cobalt atoms. Therefore, the best systems seem to be the B-site substituted $LaCoO_3$, with B cations (M^{2+} or M^{4+}) having stable oxidation states. Taking into account the appropriate sizes of B cations, Mg^{2+} and Ti^{4+} can be used to tune the oxidation state of cobalt. Substitution of Co^{3+} by Mg^{2+} formally leads to a partial oxidation of Co^{3+} towards Co^{4+}, while Ti^{4+} leads to a partial reduction towards Co^{2+}. Such compounds like $LaCo_{1-x}Mg_xO_3$ (LCMO) and $LaCo_{1-x}Ti_xO_3$ (LCTO) are known, although, the former one has a quite limited homogeneity range, $x \leq 0.1$.[1] The substitution of Co^{3+} by Mg^{2+}, with a simultaneous formation of Co^{4+}, leads to the introduction of holes accompanied by a considerable decrease of the activation energy for the electronic conductivity, similar to what has been observed upon substitution of La^{3+} by Sr^{2+} in $La_{1-x}Sr_xCoO_3$.[22] This is reflected as a decreasing positive (p-type conductivity) Seebeck coefficient with increasing Mg^{2+} content.[1] When it comes to the substitution of Co^{3+} by Ti^{4+} in LCTO, several studies[1,2,23,24] have shown that it is possible to substitute up to an x value of 0.5, corresponding to the presence of Co^{2+} ions only. The conductivity for LCTO decreases with x, but changes first from p-type for $LaCoO_3$ to n-type, and then later back to p-type when x exceeds 0.1. This unexpected behaviour has been attributed to the decrease in electron mobility due to trapping of electrons in Ti^{4+}–O–Co^{2+} clusters.[1] It can be added here that TECs have not been determined for the LCTO and LCMO systems to date, although it might be of interest, when investigating the effects of a varying oxidation state of Co. However, for $LaCo_{1-x}M_xO_3$ the cobalt content changes with M cation content (x) making it difficult to distinguish between effects on the electronic transport properties caused by changes in the cobalt oxidation state from those caused by changes in the cobalt content. For the LCMO system the formation of oxygen vacancies upon Mg^{2+} substitution is an additional complexity.[1]

Compounds in the system $La_2Co_{1+z}(Ti_{1-x}Mg_x)_{1-z}O_6$ are excellent candidates for studying correlations between cobalt oxidation state and various high-temperature properties. One of the reasons for this is that the oxygen content of $La_2Co(Ti_{1-x}Mg_x)O_6$ remains unchanged up to high-temperature regions. This conclusion is supported by the absence of the weight change of the $La_2Co(Ti_{0.5}Mg_{0.5})O_6$ sample in thermogravimetric experiment in a vacuum (~10^{-3} bar) up to 1273 K. In addition, thermogravimetric measurements in air from room temperature up to 1173 K of samples with $x = 0.0$, 0.3 and $x = 0.5$ with $z = 0.4$ showed no furthermore changes in weight ($\ll$0.5 wt%). However, during high temperature measurements of the magnetic susceptibilities in a PPMS instrument under high vacuum (10^{-8} bar), hysteresis effects were observed for the heating and cooling curves of the magnetic susceptibility.[15] After such measurements, the X-ray powder diffraction patterns of the $x = 0.5$ with $z = 0.2$ sample resulted in a significant increase in the unit cell volume from 344.37 Å^3 to 349.04 Å^3, which changed back to the original value after heating in air at 973 K. This shows that in air, at least for $La_2Co(Ti_{1-x}Mg_x)O_6$, one can exclude the effect of the so-called chemical factor, associated with the formation of oxygen vacancies at high temperatures, which has an influence on both transport and thermal expansion properties of oxides. The absence of oxygen vacancies in such type of cobaltites can also be supported by the results of the recent study of $La_{2-x}Sr_xCoTiO_6$, $0 \leq x \leq 1.0$, where the authors did not observe the deviation from the oxygen stoichiometry for the whole compositional range in air atmosphere.[9] The probability of oxygen vacancies at elevated temperatures for the Co-rich compositions $La_2Co_{1+z}(Ti_{0.5}Mg_{0.5})_{1-z}O_6$, $z = 0.2$, 0.4 and 0.6, as in the case of $LaCoO_3$,[25,26] is significantly higher, of course. However, there were no indications of the formation of oxygen vacancies in the compounds under the studied experimental conditions.

Based on the obtained results of high-temperature property measurements of $La_2Co_{1+z}(Ti_{1-x}Mg_x)_{1-z}O_6$ samples, such as thermal expansion, electronic conductivity, and Seebeck coefficient, the samples gather in 3 different groups of behaviour. The first group includes the $La_2Co(Ti_{1-x}Mg_x)O_6$, $x = 0.0$ and 0.1 samples, which differ compared to the other compositions in their thermal expansion behaviour and electronic conductivity properties (see Fig. 1, 3 and 5). This is due to the fact that $x = 0.0$ and 0.1 samples have the highest amount of Co^{2+} and, more importantly, Ti and Co are ordered in their crystal structures.[15] It should be mentioned here that the B-cation ordering is also found for the $x = 0.2$ sample, however, the ordering is weaker than for $x = 0.0$ and 0.1 as judged from the SAED patterns and the Néel temperature (T_N ($x = 0.2$) ≈ 8 K compared to T_N ($x = 0.1$) ≈ 15 K).[15] The second group includes $La_2Co(Ti_{1-x}Mg_x)O_6$, $x = 0.2$–0.4 samples, where the lattice symmetry changes from monoclinic to orthorhombic with increasing x, the latter with complete disorder of the B-cations. The third group includes compositions $La_2Co_{1+z}(Ti_{0.5}Mg_{0.5})_{1-z}O_6$, $z = 0.2$–0.6 with only Co^{3+}. The composition $La_2Co(Ti_{0.5}Mg_{0.5})O_6$ is difficult to appoint to the second or the third group. According to the thermal expansion and high-temperature conductivity behaviour it belongs to the second group, while according to Seebeck coefficient measurements it is better to refer it to the third group.

In the discussion one should also remember that the XANES studies suggest that cobalt exists in two discrete oxidation states *i.e.* Co^{2+} and Co^{3+}. To understand high-temperature properties of the compounds in such systems it is necessary to take into account transitions between LS and HS states of Co^{3+} as well as the disproportionation of Co^{3+} to Co^{4+} and Co^{2+}. We will not involve the possibility of IS Co^{3+} in our discussions as it is not necessary and the presented results do not add something to the ongoing discussion in the literature on whether IS Co^{3+} exists or not in cobalt-based perovskites.

4.1. Thermal expansion coefficients

The major contribution to the increasing average TEC of $La_2Co(Ti_{1-x}Mg_x)O_6$ with x seems to originate from the formation of Co^{3+} ions when Mg^{2+} is introduced, since the number of oxygen vacancies are negligible and the structural changes are not drastic.[15] One may therefore expect that the main contribution to the thermal expansion comes from transitions between different spin states of Co^{3+}.

The thermal expansion curve for the sample with composition $x = 0.0$, with HS Co^{2+} shown in Fig. 1, follows a straight line, as anticipated from a material where the main expansion comes from thermal vibrations. This composition can therefore be considered as the baseline for the thermal expansion of the compounds. When the Co^{3+} content in $La_2Co(Ti_{1-x}Mg_x)O_6$ increases with increasing x, the linear relation between thermal expansion and temperature disappears and the curves start to bend upwards at high temperatures, as seen in Fig. 1. This non-linearity can be explained by spin transitions of LS to HS Co^{3+}. The average TEC calculated between $T = 298$ and 1273 K increases fairly linearly with increasing x, *i.e.* with increasing relative content of Co^{3+}, from ~9 ppm K^{-1} for $x = 0.0$ to ~19 ppm K^{-1} for $x = 0.5$, as shown in Fig. 3. The TEC values (*ca.* 21 ppm K^{-1}) for $La_2Co_{1+z}(Ti_{0.5}Mg_{0.5})_{1-z}O_6$, $z = 0.2$, 0.4 and 0.6 with Co oxidation state 3+ only are slightly higher than those for the sample with $z = 0.0$ (*ca.* 19 ppm K^{-1}) and close to the value 21 ppm K^{-1} (ref. 27) reported for $LaCoO_3$, *cf.* Fig. 3.

The increase in TEC from $x = 0.0$ to $x = 0.3$ is an order of magnitude smaller than what is observed for $x > 0.3$. This can be explained by taking into account the different proportions of LS and HS Co^{3+} in the samples with different Mg^{2+} contents. The XANES measurements showed that the LS/HS ratio increases as the x-value increases.[15] The stabilization of LS Co^{3+} with an increase of the Mg^{2+} amount can easily be explained by the so-called chemical pressure effects, which is caused by the presence of the larger Mg^{2+} neighbouring the Co^{3+} cations. It resembles the situation with the spin blockade phenomenon which takes place in $La_{1.5}Sr_{0.5}CoO_4$, where ordering of large Co^{2+} (HS) and Co^{3+} causes the latter to stabilize in a LS state with smaller ionic radius[28] Therefore, one can expect an increase in the amount of LS Co^{3+} with increasing magnesium content, leading to an accelerating effect of Co^{3+} LS/HS spin transitions upon thermal expansion of $La_2Co(Ti_{1-x}Mg_x)O_6$ with increasing x. This is in agreement with the magnetic measurements, where $1/\chi$ *vs.* T for $x = 0$, 0.2 obeys the Curie–Weiss law up to 773 K, which is not the case for the $x = 0.5$ sample with nominally only Co^{3+} (Fig. 9 and 10). The former results imply that there are no major changes in the spin states of Co^{2+} and Co^{3+} with temperature for the $x = 0.0$ and 0.2 samples, while for $x = 0.5$ LS to HS transition upon heating is clearly seen as changes in the magnetic susceptibility. The obtained magnetic moments for $x = 0.2$ and 0.5 correspond to that for the $x = 0.2$ sample containing ~84% of HS Co^{3+}, while the $x = 0.5$ sample contains ~57% of HS Co^{3+} at 800 K.

With the decrease of the (Mg,Ti)/Co ratio in $La_2Co_{1+z}(Ti_{0.5}Mg_{0.5})_{1-z}O_6$, with $z = 0.2$–0.6, the effect of changing the Mg/Ti-cation content on the spin state of Co^{3+} becomes weaker. Therefore the spin state of Co^{3+} at certain compositions becomes only temperature dependent. The TECs for $z = 0.2$, 0.4 and 0.6 are very similar and correspond to what has been observed for $LaCoO_3$.[13] Obviously, the effect of Co^{3+} spin-transitions on the TEC gets saturated for 60% ($z = 0.2$) of Co^{3+} at the B-site. Thus, for the compositions with different amounts of total Co^{3+}, the spin-state transitions of the Co^{3+} ions do not add up into large TECs as a linear accumulation. The structural changes for the rhombohedral $La_2Co_{1+z}(Ti_{0.5}Mg_{0.5})_{1-z}O_6$ compounds with z are obviously too small to be seen in the TEC.

4.2. Electronic conductivity and Seebeck measurements

The electronic conductivities of the compounds increase both with increasing Co^{3+}/Co^{2+} ratio for $La_2Co(Ti_{1-x}Mg_x)O_6$ and with increasing total Co^{3+} content in $La_2Co_{1+z}(Ti_{0.5}Mg_{0.5})_{1-z}O_6$. Even at high temperatures where the difference in conductivities between different compositions becomes smaller, this trend is clearly seen as depicted in the right part of Fig. 4. From the decreasing Seebeck coefficients with increasing amount of Co^{3+} it is clear that this is due to a simultaneous increase of the number of charge carriers. The Seebeck coefficients are positive for all compositions in the whole studied temperature range except for the $La_2Co_{1.6}(Ti_{0.5}Mg_{0.5})_{0.4}O_6$ sample that becomes negative at $T < 390$ K. Therefore all the studied compounds are p-type conductors, except the latter one at $T < 390$ K.

For the first group of compositions ($La_2Co(Ti_{1-x}Mg_x)O_6$, $x = 0.0$ and 0.1) mentioned above, the Seebeck coefficient is relatively high and positive, although Ti^{4+} should be an n-type dopant. This result is in agreement with what was reported for La_2CoTiO_6 ($x = 0.0$) by Nakatsugawa and Iguchi[29] and $LaCo_{1-x}Ti_xO_3$, $x = 0.01$, 0.1 and 0.2 by some of us.[2] The p-type conduction is obtained as the electrons become trapped by the extra bands created by Ti^{4+} impurity levels when Ti^{4+} is abundant and ordered in the structure and the electron mobilities thus decrease.[30,31] The temperature dependence of the conductivity for the first group of compositions exhibits a semiconducting behaviour with constant activation energy over the whole studied temperature range. It should be mentioned that activation energies of conductivities for samples belonging to the first group are by *ca.* 30% lower in comparison with the first compositions ($x = 0.2$ and 0.3) of the second group (Fig. 4, left side), therefore reflecting the importance of the B-cation disorder effect. It is attributed to an increased difficulty for the charge carriers to jump between different sites in the crystal, mainly due to an increasing probability of having a Mg^{2+} ion nearby a Co ion. This would hinder the small polarons, resulting in larger activation energies.

For the second group of compositions, with complete disorder on the B-cation site, an increase in conductivity and a decrease in the average activation energy with an increase of the Mg^{2+} content are observed (Fig. 4). The charge-carrier concentration increases as the amount of Co^{3+} increases as can be observed from measurements of the Seebeck coefficient. The non-linear behaviours of the conductivities observed at higher temperatures are due to the decrease of the activation energy. It starts around $T = 973$ K for $x = 0.2$ where the change is rather small, but for the samples with $x > 0.3$ it is significant and shifts to lower temperatures with increasing x. It can be ascribed to the temperature dependence of the disproportion reaction of Co^{3+}. It is known that the conductivity in Co^{3+} containing perovskites is promoted by disproportionation according to the reaction equation $2Co^{3+} \rightarrow Co^{2+} + Co^{4+}$. The disproportionation equilibrium is further shifted to the right side for Co^{3+} in the HS state.[17] It should be mentioned that the equilibrium constant of this reaction, $K = \frac{[Co^{2+}][Co^{4+}]}{[Co^{3+}]^2}$, increases with temperature. The equilibrium of the disproportionation reaction is shifted towards the Co^{3+} side for $La_2Co(Ti_{1-x}Mg_x)O_6$ in comparison with undoped $LaCoO_3$ due to the presence of Co^{2+} and to the increasing proportion of LS Co^{3+}, as mentioned above. It is obvious that the proportion of Co^{2+}/Co^{3+} and the LS/HS ratio for Co^{3+} change in opposite directions with x. However, the decrease of the upper temperature limit for the linear behaviour of the conductivity *vs.* temperature with increasing Co^{3+} (x) shows that the Co^{2+}/Co^{3+} ratio is more important in the case of $La_2Co(Ti_{1-x}Mg_x)O_6$ perovskites.

For the third group of compositions with only Co^{3+} a large increase in conductivity together with a decrease of activation energy occurs with increasing cobalt content. This can be explained by an expansion of the conductive network of Co^{3+} ions on the way to $LaCoO_3$. Moreover, trends in temperature dependences of both conductivity and Seebeck coefficient are similar to those for substituted $LaCoO_3$. At $T < 473$ K, low ($z = 0.4$) or even small negative ($z = 0.6$) Seebeck coefficients are observed, which can be related to an increased or even higher mobility of the electrons than found for the holes at lower temperatures.[29,32–35] This resembles the behaviour of n-doped $LaCoO_3$ (*i.e.* slightly oxygen deficient $LaCoO_{3-\delta}$ after treatment in reducing atmosphere or by Ti^{4+} doping).[33,34] The Seebeck coefficients then increase with temperature as the electrons are recombining with the holes formed. This reaches a maximum at $T \approx 653$ K, after which it decreases again as the number of hole carriers continues to increase by the formation of charge carriers through disproportionation of Co^{3+} to Co^{4+} and Co^{2+}. At higher temperatures the Seebeck coefficients of the samples with $x = 0.5$ along the $La_2Co_{1+z}(Ti_{0.5}Mg_{0.5})_{1-z}O_6$ series converge towards a positive value in the range 35–50 μV K^{-1} at $T \approx 1173$ K. This is similar to what has been reported for slightly n-doped $LaCoO_3$.[2,33,34]

5. Conclusions

The studied system $La_2Co_{1+z}(Ti_{1-x}Mg_x)_{1-z}O_6$ represents a rare example of Co-containing perovskites with 3D octahedral network, where it is possible to study correlations between cobalt oxidation state only and various high-temperature properties of importance for gas separation membranes and different high temperature electrochemical devices *e.g.* SOFCs. Based on the temperature dependence of the thermal expansion, electronic transport properties and Seebeck coefficients, three different groups of compositions can be allocated. The first group is $La_2Co(Ti_{1-x}Mg_x)O_6$, $x = 0.0$ and 0.1 with ordered Co^{2+} and Ti^{4+} cations in the crystal structure. The second group includes samples of $La_2Co(Ti_{1-x}Mg_x)O_6$, $x = 0.2$–0.4, while the third one merges compositions $La_2Co_{1+z}(Ti_{0.5}Mg_{0.5})_{1-z}O_6$, $z = 0.2$–0.6 with Co^{3+}-only. We did not observe any influence from the detailed crystal structures (except the ordering at the B-site for $x \leq 0.2$) like changes in tilting of the octahedra on the studied high-temperature properties. The thermal expansion behaviours of the studied compounds are mainly dependent on the proportion of Co^{2+}/Co^{3+}. For $La_2Co(Ti_{1-x}Mg_x)O_6$, the TEC increases from ~9 ($x = 0$) to 19 ppm K^{-1} ($x = 0.5$) with an increase of the oxidation state of cobalt from +2 to +3, respectively. However, the increase is not linear with increasing Co^{3+} content because the LS/HS ratio for Co^{3+} is dependent on the magnesium content. The main reason for this is the so-called chemical pressure effect caused by the presence of large Mg^{2+} on the neighbouring Co^{3+}. This conclusion is supported by magnetic susceptibility measurements performed on samples with different oxidation states of cobalt. The thermal expansion of $La_2Co_{1+z}(Ti_{0.5}Mg_{0.5})_{1-z}O_6$, $z = 0.2$–0.6 with Co^{3+}-only remains constant at ~21 ppm K^{-1} independent of the cobalt content. All the studied compounds present p-type conductivity, except $La_2Co_{1.6}(Ti_{0.5}Mg_{0.5})_{0.4}O_6$ at $T < 390$ K. The electronic conductivities were found to increase with an increase of both Co^{3+} and total cobalt content and are described using a small polaron hopping model.

Acknowledgements

The authors want to thank the Visbyprogramme at Swedish Institute, Swedish research council, SNF (Swiss National Science Foundation) and the Ministry of Science and Education of Russian Federation (state contract 14.740.12.1358) for financial support. The authors are grateful to E. Brücher for measurement of the magnetic data.

References

1 N. Ramadass, J. Gopalakrishnan and M. V. C. Sastri, *J. Less Common Met.*, 1979, **65**, 129–138.
2 R. Robert, L. Bocher, M. Trottmann, A. Reller and A. Weidenkaff, *J. Solid State Chem.*, 2006, **179**, 3893–3899.
3 A. Podlesnyak, K. Conder, E. Pomjakushina, A. Mirmelstein, P. Allenspach and D. Khomskii, *J. Magn. Magn. Mater.*, 2007, **310**, 1552–1554.

4 P. G. Radaelli and S.-W. Cheong, *Phys. Rev. B: Condens. Matter*, 2002, **66**, 1–9.

5 D. Tsvetkov, A. Zuev, A. Vylkov and A. Petrov, *Solid State Ionics*, 2007, **178**, 1458–1462.

6 Z. Y. Wu, M. Benfatto, M. Pedio, R. Cimino, S. Mobilio, S. R. Barman, K. Maiti and D. D. Sarma, *Phys. Rev. B: Condens. Matter*, 1997, **56**, 2228–2233.

7 M. Korotin, S. Ezhov, I. Solovyev, V. Anisimov, D. Khomskii and G. Sawatzky, *Phys. Rev. B: Condens. Matter*, 1996, **54**, 5309–5316.

8 H. Nakao, T. Murata, D. Bizen, Y. Murakami, K. Ohoyama, K. Yamada, S. Ishiwata, W. Kobayashi and I. Terasaki, *J. Phys. Soc. Jpn.*, 2011, **80**, 023711.

9 M. Yuste, J. C. Pérez-Flores, J. R. de Paz, M. T. Azcondo, F. García-Alvarado and U. Amador, *Dalton Trans.*, 2011, **40**, 7908–7915.

10 F. Fauth, E. Suard and V. Caignaert, *Phys. Rev. B: Condens. Matter*, 2001, **65**, 2–5.

11 M. W. Haverkort, Z. Hu, J. C. Cezar, T. Burnus, H. Hartmann, M. Reuther, C. Zobel, T. Lorenz, A. Tanaka, N. B. Brookes, H. H. Hsieh, H.-J. Lin, C. T. Chen and L. H. Tjeng, *Phys. Rev. Lett.*, 2006, **97**, 38–41.

12 A. Petric, P. Huang and F. Tietz, *Solid State Ionics*, 2000, **135**, 719–725.

13 S. Uhlenbruck and F. Tietz, *Mater. Sci. Eng., B*, 2004, **107**, 277–282.

14 A. Petric, P. Huang and F. Tietz, *Solid State Ionics*, 2000, **135**, 719–725.

15 S. Shafeie, J. Grins, S. Y. Istomin, L. Karvonen, S. a. Chen, T. H. Chen, J. M. Chen, A. Weidenkaff, M. Karppinen and T. Sirtl, *J. Solid State Chem.*, 2011, **184**, 177–190.

16 M. Radovic, S. a. Speakman, L. F. Allard, E. a. Payzant, E. Lara-Curzio, W. M. Kriven, J. Lloyd, L. Fegely and N. Orlovskaya, *J. Power Sources*, 2008, **184**, 77–83.

17 R. Koc and H. U. Anderson, *J. Eur. Ceram. Soc.*, 1995, **15**, 867–874.

18 J. B. Goodenough, *Mater. Res. Bull.*, 1970, **5**, 621–629.

19 A. N. Petrov, A. Y. Zuev, A. I. Vylkov and D. S. Tsvetkov, *Russ. J. Phys. Chem.*, 2006, **80**, S128–S133.

20 J. Lago, P. D. Battle, M. J. Rosseinsky, A. I. Coldea and J. Singleton, *J. Phys.: Condens. Matter*, 2003, **15**, 6817–6833.

21 M. A. Hayward and M. J. Rosseinsky, *Chem. Mater.*, 2000, **12**, 2182–2195.

22 P. Ravindran, P. A. Korzhavyi, H. Fjellvåg and A. Kjekshus, *Phys. Rev. B: Condens. Matter*, 1999, **60**, 16423–16434.

23 R. Robert, D. Logvinovich, M. H. Aguirre, S. G. Ebbinghaus, L. Bocher, P. Tomeš and A. Weidenkaff, *Acta Mater.*, 2010, **58**, 680–691.

24 I. Álvarez-Serrano, G. J. Cuello, M. L. López, A. Jiménez-López, C. Pico, E. Rodríguez-Castellón, E. Rodríguez and M. L. Veiga, *J. Phys. D: Appl. Phys.*, 2008, **41**, 195001.

25 S. Yamauchi, T. Ishigaki, J. Mizusaki and K. Fueki, *Solid State Ionics*, 1983, **9–10**, 997–1000.

26 L. B. Sis, G. P. Wirtz and S. C. Sorenson, *J. Appl. Phys.*, 1973, **44**, 5553–5559.

27 V. V. Kharton, F. M. Figueiredo, A. V. Kovalevsky, A. P. Viskup, E. N. Naumovich, A. A. Yaremchenko, I. A. Bashmakov and F. M. B. Marques, *J. Eur. Ceram. Soc.*, 2001, **21**, 2301–2309.

28 C. F. Chang, Z. Hu, H. Wu, T. Burnus, N. Hollmann, M. Benomar, T. Lorenz, A. Tanaka, H.-J. Lin, H. H. Hsieh, C. T. Chen and L. H. Tjeng, *Phys. Rev. Lett.*, 2009, **102**, 1–4.

29 H. Nakatsugawa and E. Iguchi, *J. Phys.: Condens. Matter*, 1999, **11**, 1711–1722.

30 P. M. Raccah and J. B. Goodenough, *J. Appl. Phys.*, 1968, **39**, 1209.

31 J. B. Goodenough, *Czech. J. Phys.*, 1967, **17**, 304–336.

32 D. Bahadur and O. Parkash, *J. Solid State Chem.*, 1983, **46**, 197–203.

33 J. Hejtmánek, Z. Jirák, K. Knížek, M. Marysko, M. Veverka and C. Autret, *J. Magn. Magn. Mater.*, 2008, **320**, e92–e95.

34 Z. Jirák, J. Hejtmánek, K. Knížek and M. Veverka, *Phys. Rev. B: Condens. Matter Mater. Phys.*, 2008, **78**, 1–8.

35 S. Hebert, D. Flahaut, C. Martin, S. Lemonnier, J. Noudem, C. Goupil, A. Maignan and J. Hejtmanek, *Prog. Solid State Chem.*, 2007, **35**, 457–467.